ELSEVIER

Atmospheric Research 63 (2002) 101–121

ATMOSPHERIC RESEARCH

www.elsevier.com/locate/atmos

Modeling surface energy fluxes for Iperó, SP, Brazil: an approach using numerical inversion

Admir Créso Targino [a,*], Jacyra Soares [b]

[a] Instituto de Computación, Centro de Cálculo, Facultad de Ingeniería, Montevideo, Uruguay
[b] Department of Atmospheric Sciences, University of São Paulo, São Paulo, Brazil

Received 4 December 2001; received in revised form 20 February 2002; accepted 22 February 2002

Abstract

The numerical surface energy-budget model proposed by Deardorff [J. Geophys. Res. 83(C4) (1978) 1899] is used to simulate surface fluxes of sensible and latent heat and net irradiance for two periods of the year in Iperó, SP, Brazil: winter of 1992 and summer of 1993. Surface energy models are very sensitive to the soil–vegetation parameters. The values of these parameters, however, are not easy to obtain. Here, a new approach to obtain a set of representative values of soil–vegetation parameters is done by using inverse modeling. The parameter values obtained by the inversion model and used in the numerical model to simulate the fluxes have provided a good description of the interface soil–vegetation conditions in Iperó, according to statistical indicators employed to evaluate the agreement between observed and simulated fluxes. The final results indicate that the inversion method is a fast and efficient resource to obtain the parameters of a model when it is not otherwise possible to get reliable reference values for numerical simulations.

Keywords: Turbulent fluxes; Estimated parameters; Soil–atmosphere interaction; Optimization technique; Inverse model

1. Introduction

The planetary boundary layer (PBL) plays an important role in the life of Earth. All human and biologic activities take place in the PBL. This represents a good reason to develop research about the physical processes of this region, where physical features are very different from the others regions of the atmosphere. Meteorologists have invested in

* Corresponding author. Currently at the Department of Meteorology, Stockholm University, S-106 91 Stockholm, Sweden. Tel.: +46-8-16-24-04.

E-mail address: admir@misu.su.se (A.C. Targino).

PII: S0169-8095(02)00025-X

developing models of land surface processes for use in climate simulations, numerical weather prediction, and air quality assessments. These efforts are necessitated by the growing demand for a better understanding of climate processes over the land surface, which must be studied in considerable detail because of their importance for food production, use of water resources, ecological processes, and other human activities.

There are several sophisticated soil–vegetation schemes that provide realistic representations of land surface–atmosphere exchange processes in meteorological models. However, using these schemes requires specifying several input parameters, not always available, to properly represent the characteristic of the land surface.

The correct specification of the turbulent fluxes represents an important point for the numerical modeling work, and because of that many authors have already devoted attention to the sensitivity of surface fluxes to the values of various important parameters (Mihailovic and Kallos, 1997; Mihailovic et al., 1992; Ookouchi et al., 1984; Anthes, 1984; McCumber, 1980). The vertical turbulent fluxes of latent and sensible heat and momentum define the lower boundary conditions of mesoscale models (Bougeault, 1991). The surface sensible heat flux is a prime forcing mechanism of the PBL thermal characteristics. Therefore, the partition of energy between the sensible and the latent heat fluxes at the surface (i.e., the Bowen ratio) is a key factor in the development of the PBL. The exchanges and forcing present in the PBL and the availability of humidity for evapotranspiration also constitute important information for both meso-scale and large-scale numerical simulations. For example, Shukla and Mintz (1982) showed that altering the amount of soil moisture might have large effects on the climate of the continents. The soil moisture through the release of turbulent latent heat flux from bare soil or a canopy modulates the magnitude of the predicted turbulent sensible heat flux. Deardorff (1978) (henceforth D78) showed that vegetation and soil moisture parameterizations significantly alter surface parameters such as temperature and turbulent fluxes. McCumber and Pielke (1981) found that vegetation and the soil moisture distribution affect the mesoscale circulation patterns, thus affecting model predictions of precipitation and other meteorological features. Mihailovic et al. (1992) used observations over a maize field to show that the fractional vegetation cover and bare soil texture alter the diurnal forcing of meteorological parameters. At mesoscale resolutions, Jacquemin and Noilhan (1990) carried out a sensitivity study using the HAPEX-MOBILHY data (André et al., 1986). They found the following order of importance for surface parameters: soil moisture, vegetation cover, minimum stomatal resistance, leaf area index, and surface roughness.

All these studies lead to the conclusion that it is necessary to improve the representation of land-surface processes and the prescription of the surface parameters because they may induce significant discontinuities in surface thermal forcing, and consequently, mesoscale circulations. Such circulations may play an important role in patterns relating to local meteorology, cumulus convection, and air quality.

Describing a set of parameters prescribing with accuracy the surface characteristics represents a very important part of numerical simulations. However, it is still a hard task. To specify the values of vegetation cover parameters, for example roughness parameter, leaf area index, vegetation albedo, among others, one employs either values from the literature or employs experimental values gathered from micrometeorological experiments. Unfortunately, the reference values available do not always suit the cases that one desires to research; and the observational campaigns are expensive to carry out regularly, which makes them even more unlikely to happen. This is the reason why we switched to a new approach to the problem to estimate adequate and representative values of the parameter: a technique known as "Numerical Inversion" or "Optimization".

Inversion problems arise when the structure of a physical system is to be identified on the basis of observations of its output. In this work, the estimation of the parameters involves optimizing the D78 model output against measured fluxes by iteratively changing a set of input parameters. The optimization procedure provides a set of parameters which gives the best match between simulated and observed fluxes.

One of the first works testing numerical inversion with micrometeorological data was carried out by Sellers et al. (1989), who used heat flux data gathered in the Amazon rainforest to calibrate the SiB model of Sellers et al. (1986). The results showed that many reference values of parameters (e.g., leaf area index, vegetation cover, among others) collected from the literature did not properly represent the environment and therefore generated a poor model of the sensible and latent heat fluxes. The numerical inversion employed by Sellers et al. (1989) proved to be very efficient in re-defining a set of values more representative of the area studied. In that case, the use of the optimized parameters in the SiB led to better agreement between the observed and simulated latent and sensible heat fluxes.

In the present work, the model proposed by D78 is employed to simulate the turbulent fluxes in a surface with vegetation, located in Iperó, Brazil. This model have been used by a number of authors in works that had various approaches (Oliveira et al., 1998; Soares et al., 1996; Targino, 1999). The main objectives of this paper are (i) to employ the D78 model to simulate energy budgets for Iperó for two different periods of the year, summer and winter; (ii) to employ numerical inversion to estimate new values for the parameters of D78; (iii) to evaluate objectively the results obtained by the inversion technique using a statistical test.

A brief description of the data is given in Section 2. Modeling aspects pertinent to the current study are given in Section 3. Statistical tools employed to evaluate the results are described in Section 4. The results are described in Section 5.

2. Data and region of study

The data used in this work were obtained at the Brazilian Navy's industrial installation Centro Experimental ARAMAR (CEA). The CEA is located at Iperó in a country region of the State of São Paulo, Brazil (23°25′ S, 47°35′ W), approximately 120 km from the Atlantic Ocean coastline and 550 m above mean sea level, as shown in Fig. 1. The site is located in the central area of the Tietê River valley, which is crossed by the Sorocaba River in a NW–SE direction. The main topographic feature is the 900-m high Araçoiaba Hill in the southwest.

The area has been the subject of two field campaigns. The campaigns took place during the winter, in July–August 1992, and in the summer, in March 1993. The surface was covered by short grass 0.2-m high in July–August and by corn 0.5-m high in March. Table 1 describes the field campaigns employed in this work.

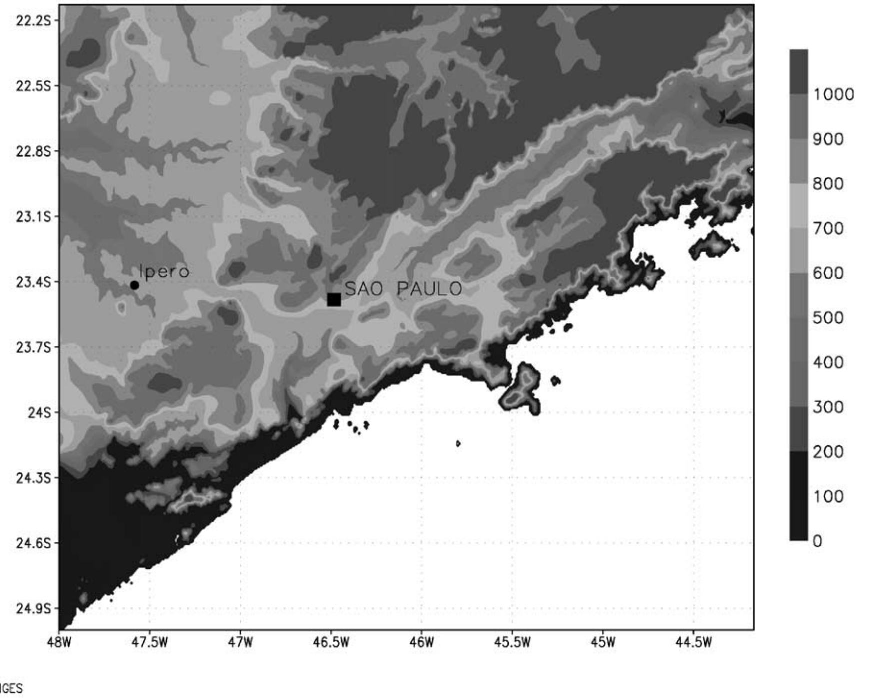

Fig. 1. Map indicating the topography of the eastern part of the state of São Paulo, Brazil. Iperó is 120 km from the shoreline and 80 km from the city of São Paulo (also plotted). The topography data have a 1 × 1-km resolution (data source: Department of Geophysics, University of São Paulo, Brazil).

2.1. Available data

During the field campaigns, surface-layer turbulence data were obtained using a micrometeorological tower 12-m high with sensors installed at different levels, as described below.

- Fluctuations of vertical velocity, temperature, and water vapor density at three fixed levels: 3.0, 5.0, and 9.4 m above surface.
- Air temperature and relative humidity at three levels: 2.0, 4.0, and 8.8 m, during the winter experiment of 1992; 2.0, 5.0 and 10.0 m, during the summer experiment of 1993.

Table 1
Description of the experiments used in this study

Period of the campaign	Day studied	Experiment	Type of the surface where the micrometeorological tower was installed
July 28–August 07, 1992	August 07, 1992	Winter	Grass, 20 cm high
March 08–21, 1993	March 12, 1993	Summer	Corn in growing phase, 50 cm high

- Air temperature, relative humidity and atmospheric pressure at surface level.
- Ground temperature at three levels below the surface: 1.0, 8.0, and 15.0 cm.
- Soil heat flux at two levels: 1.0 and 8.0 cm.
- Soil moisture at 4.0 cm.
- Net irradiance.
- Global, direct, and surface reflected irradiance.
- Morphological and thermal properties of the soil.
- Horizontal wind speed and direction (zonal component), at 11 m, during the winter experiment; wind speed and direction (zonal and meridional components) at 11.5 m, during the summer experiment.

Temperature was measured with HMP25C thermometers manufactured by Vaisala (with an accuracy of 0.4 °C); relative humidity was measured with HMP35C hygrometer manufactured by Vaisala (with an accuracy of 2%), both with a time response of 15 s. Propeller anemometers of the R.M. Young were used to measure the zonal and meridional components of wind velocity.

A sonic anemometer, a fine wire thermometer, and a krypton hygrometer were used to measure, respectively, perturbations of vertical velocity (w', with an accuracy of 0.05 m s^{-1}), temperature (T', with an accuracy of 0.2 °C), and water vapor density (q', with an accuracy of 0.02 g m^{-3}). The turbulence data were sampled at a frequency of either 1 or 10 Hz and the covariance reported here was evaluated using 20-min averaging periods. The data set was interpolated in time using a convergent weighted-averaging interpolation scheme (Barnes, 1964). It is based on the supposition that the distribution of an atmospheric variable at any given time can be represented by the summation of an infinite number of independent waves, i.e., a Fourier integral interpolation. Further information about instrumentation and collected data can be found in Oliveira (1993).

To characterize the seasonal variation of the PBL, the data of August 7, 1992 (Julian day 219) were taken as being representative of winter conditions. The summer conditions were represented by the data of March 12, 1993 (Julian day 71). We will refer to them as the *winter experiment* and the *summer experiment*, respectively. These days were chosen due to the availability of uninterrupted observations, characterized by no gaps in the time series of the fluxes of sensible and latent heat and net irradiance. Also, no rain was observed during these two periods, and any significant synoptic disturbance or cloud effects did not affect the local PBL time evolution.

3. The numerical models

The numerical models used in the present study consist of two modules, the so-called *forward model* and the *inverse model*.

3.1. The forward model

To apply numerical inversion, one must first find a model that simulates the generation of the data to be inverted. This model is referred to as the "forward model".

The forward model used here is that proposed by D78 and allows simulating the time evolution of the surface heat fluxes. The D78 model uses, as external forcings, measurements of air temperature, specific humidity, and wind speed sampled from meteorological observations at one level above the surface, here assumed to be 10 m (see Section 2). As internal parameters, a set of values related to the soil and vegetation is employed (Table 2). All the parameters listed in Table 2 must be assigned values prior to the operation of D78. The model includes the variability of soil properties and the influence of a vegetation cover on the exchanges between soil–vegetation and atmosphere. This parameterization has been widely used, especially in mesoscale models (e.g., McCumber, 1980; Garrett, 1982). Its formulation is described comprehensively in D78 and Bougeault (1991), and therefore only some characteristics will be outlined here.

In the method proposed by D78, a single layer of vegetation with negligible heat capacity is assumed to be present. Its horizontal density is characterized by the single quantity σ_f, which is an area-averaged shielding factor associated with the degree to which the foliage prevents short wave radiation from reaching the ground. Its value ranges between 0 and 1. $\sigma_f = 0$ corresponds to the bare soil case, and $\sigma_f = 1$ corresponds to complete radiative blocking.

The air in close proximity to the foliage is assumed to have properties intermediate among the above-canopy air, the foliage surface, and the ground surface. In this case, three different determinations of the temperature and the humidity are considered.

Air properties: T_a and q_a represent the temperature and humidity of the air above the canopy (measured at 'anemometer' reference level z_a).

Ground surface properties: T_g is the ground surface temperature that is determined following Bhumralkar (1975) and Blackadar (1976). The determination of T_g basically involves a numerical solution of an abbreviated surface energy budget equation (force-restore method). They showed that it is possible to achieve qualitatively good results for the prediction of T_g if the soil is divided into only two layers: one surface layer of very small depth (typically 10 cm) that follows the diurnal cycle, and one deep layer (typically 1 m) that follows the annual cycle. The surface value of the soil temperature T_g is

Table 2
Input parameters required by D78

Symbol	Definition	Unit
z_0	Roughness length	m
z_{0h}	Canopy roughness length	m
d	Displacement height	m
σ_f	Foliage shielding factor	–
ε_f	Foliage emissivity	–
ε_g	Ground surface emissivity	–
α_f	Foliage albedo	–
K_s	Soil thermal diffusivity	$m^2\ s^{-1}$
w_{wilt}	Wilting value of w	$m^3\ m^{-3}$
w_k	Critical or saturated value of w	$m^3\ m^{-3}$

predicted by a simple equation that includes a restoring term containing the deep soil temperature T_2

$$\partial T_g/\partial t = -c_1 H_A/(\rho_s c_s d_1) - c_2(T_g - T_2)/\tau_1 \tag{1a}$$

$$\partial T_2/\partial t = -H_A/(\rho_s c_s d_2) \tag{1b}$$

where T_2 is the mean soil temperature over a layer of depth d_2; H_A is the sum of fluxes toward the atmosphere; c_1 and c_2 are dimensionless constants; ρ_s is the density of the soil; c_s is the specific heat of the soil; d_1 and d_2 are the soil depths influenced by the diurnal and annual temperature cycles, respectively; and τ_1 is the diurnal period (24 h). The first term in Eq. (1a) expresses the atmospheric forcing, whereas the second term is seen to restore T_g exponentially toward the deep soil temperature that changes with an annual scale only.

The success of the simplified formulation based on the force-restore method for the prediction of ground surface temperature has inspired a similar effort for the prediction of ground surface moisture content. The specific humidity at the surface q_g is then related to the ground surface moisture content. Assuming that most of the vertical movement of the volumetric concentration of ground soil moisture w within the soil can be described by a diffusion process, D78 proposed a parameterization of this process based on the analogy with Eqs. (1a) and (1b)

$$\partial w_g/\partial t = -C_1(E_g + 0{,}1E_{tr})/(\rho_w d_1') - C_2(w_g - w_2)/\tau_1 \tag{2a}$$

$$\partial w_2/\partial t = -(E_g + E_{tr})/(\rho_w d_2') \tag{2b}$$

where w_g is the ground surface value of w; ρ_w is the density of liquid water; c_1 and c_2 are constants analogous to C_1 and C_2; d_1' and d_2' are typical depths influenced by the diurnal and seasonal soil moisture cycles, respectively. D78 suggested $d_1' = 10$ cm and $d_2' = 50$ cm; w_2 is the vertically averaged value of w over the layer of depth d_2'; E_g is the evaporation rate at the ground surface; E_{tr} is the foliage transpiration rate.

The ground albedo depends on the water soil content, according to Idso et al. (1975)

$$\alpha_g = 0.31 - 0.17 w_g/w_k, \qquad w_g \le w_k$$

$$\alpha_g = 0.14, \qquad w_g > w_k \tag{3}$$

Foliage surface properties: Finally, T_f and q_f are the representative temperature and moisture of the canopy itself. T_f is determined from an equilibrium energy budget of the canopy, and q_f is the equivalent moisture in the immediate vicinity of the leaves. Additionally, the properties of the air inside the canopy, T_{af} and q_{af}, are defined as empirical linear combinations of T_a, T_f, T_g and of q_a, q_f, q_g, respectively.

The air velocity inside the canopy u_{af} is taken as different from, but a function of, the air velocity outside the canopy u_a. The exchange of heat and moisture between the canopy and the atmosphere is assumed to be governed by u_{af}, $T_f - T_{af}$, $q_{sat}(T_f) - q_{af}$. Fig. 2 illustrates the problem using the notation described in Table 3.

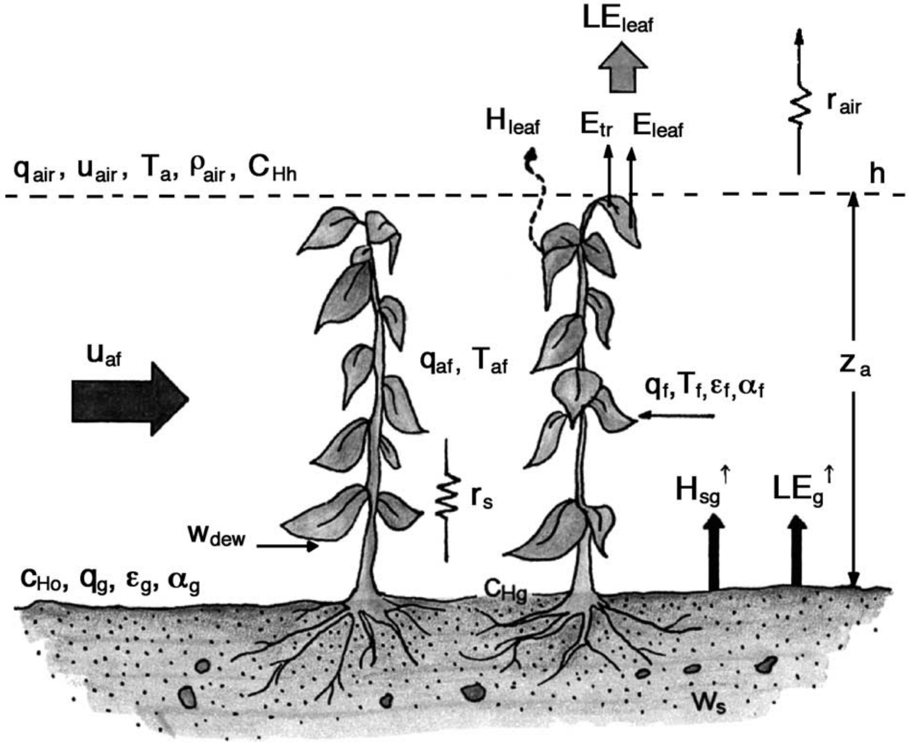

Fig. 2. Schematic representation of the parameterization described by D78 (arrow widths do not represent flux intensity).

3.2. The inverse model

Before introducing the concept of the inverse problem, we must explain what is a forward problem. The concept of a forward problem may be interpreted as a process where, from certain initial conditions, a system undergoes transformations and acquires new configurations. An inverse formulation to a problem tries to estimate the parameters of a system (boundary conditions and initial parameters), based on observed effects. A suitable definition for inverse problem, attributed to Oleg M. Aifanov, and quoted by Woodbury (1995) is "Solution of an inverse problem entails determining unknown causes based on observation of their effects. This is in contrast to the corresponding direct problem, whose solution involves finding effects based on a complete description of their causes."

3.3. Formulation of the problem

The problem approached here consists of determining of a set of parameters K used by D78, which, in this case, may be the roughness parameter z_0, vegetation emissivity ε_f,

Table 3
Notation used in Fig. 2

Symbol	Definition
d_1, d'_1	Depth of the temperature and moisture diurnal cycles, respectively
d_2, d'_2	Depth of the annual temperature cycle and seasonal moisture diurnal cycles, respectively
E_{tr}	Foliage transpiration rate
q	Specific humidity
z_o	Roughness length
d	Displacement height
z	Vertical height
r_{air}	Atmospheric resistance
r_s	Generalized stomatal resistance
T	Absolute temperature
T_2	Mean soil temperature over layer of depth d_2
u	Wind speed
w_g	Volumetric concentration of soil moisture
w_2	Soil moisture content within the layer of depth d'_2
w_{dew}	Mass of liquid water retained by foliage
w_s	Soil moisture value in the root zone
α	Albedo
ε	Emissivity
ρ_{air}	Air density
c_H	Dimensionless heat or moisture transfer coefficient
H_{leaf}	Sensible heat flux of a representative leaf
LE_{leaf}	Latent heat flux of a representative leaf
H_s	Sensible heat flux
LE	Latent heat flux
R_L	Long-wave irradiance
R_S	Short-wave irradiance
G	Soil heat flux at the surface
Subscripts	**Definition**
a	Reference 'anemometer level' height
h	Height just above the top of canopy
f	Foliage surface
a_f	Mean value of the variable within the canopy
0	Evaluation at the surface of bare soil
g	Value at the ground surface

among others (Table 2). Basically, it is possible to specify these parameters by two different ways. The first is to obtain values from the literature and perform trial-and-error tests until a suitable set of values is found; this method is the most commonly used when no reliable micrometeorological measurements are available. The second option is to use measurements of meteorological variables and surface fluxes and then to optimize the parameters for which most uncertainty exists. This involves operating the forward model in an iterative loop driven by a least-square reduction algorithm. To do that we employed time series of latent and sensible heat fluxes and net irradiance $C_{L,i}$, $C_{S,i}$ and $C_{R,i}$, where the subindices L, S, and R stand for latent heat flux, sensible heat flux, and net irradiance, respectively; $i=1,\ldots,N$, where N represents the number of observations. The mathematical approach used in this problem is made through an implicit method. An implicit method tries to adjust the mathematical solution through an interactive search process until the best agreement between observed and simulated series is reached.

In this work, the inversion problem is formulated as a non-linear optimization problem subjected to constraints. The objective is to optimize (minimize) a given function f. This function is called the objective function $R(K)$. The objective function represents the sum of the square differences between each series of calculated fluxes $C_{\mathrm{L},i}^{\mathrm{calc}}(K)$, $C_{\mathrm{S},i}^{\mathrm{calc}}(K)$, and $C_{\mathrm{R},i}^{\mathrm{calc}}(K)$ and the corresponding counterpart of experimental fluxes $C_{\mathrm{L},i}^{\mathrm{exp}}$, $C_{\mathrm{S},i}^{\mathrm{exp}}$, and $C_{\mathrm{R},i}^{\mathrm{exp}}$ obtained from the micrometeorological measurements. $R(K)$ may be written in the following way

$$R_j(K) = \sum_{i=1}^{N} (C_{\mathrm{J},i}^{\mathrm{calc}} - C_{\mathrm{J},i}^{\mathrm{exp}})^2 \tag{4}$$

where J = L, S, R and have the same meaning as above.

K=[k_1,...,k_M] represents a vector of parameters k_j to be estimated; M is the number of parameters; each parameter k_j follows $l_j \leq k_j \leq u_j$, where l_j and u_j are the upper and lower bounds of the searched parameters. These bounds restrict the domain values and specify an interval whose values are physically accepted.

Usually, these limits come from previous information about the parameters. The bounds especially in an inequality-like specification like that presented above, lead to improvements in the convergence of the optimization algorithm. The choice of appropriate l_j and u_j ensures that the inversion routine locates the parameters k_j within acceptable physical limits, keeping the algorithm from working in irrelevant response regions.

3.4. Iterative method of solution

The minimization of the objective function $R_j(K)$, subject to simple bounds on K, is solved using a first-order optimization algorithm provided by the E04UCF routine from the Numerical Algorithms Group (NAG) Fortran Library (1993). This routine is designed to minimize arbitrary smooth functions subject to constraints (simple bounds, linear, and nonlinear constraints) using a sequential programming method. To initiate the inversion process, it is necessary to have an initial guess of the desired result. In this case, trial values for the set of parameters to be estimated are input. The forward model calculates time series of heat and radiation fluxes using this first trial and compares the result with the measured series using Eq. (4). Then an updated set of parameters is obtained, which is then used to compute a new model response estimate. At each stage, the sum of the squares of the error between the model response and the observation values is monitored, so that Eq. (4) is minimized at each iteration. The iterative search for the estimated parameters terminates whenever either the squared error or a relative change in the squared error becomes less than a specified value. After these convergence criteria have been satisfied, we may say that the estimated values of the soil–vegetation parameters have produced a suitable description of the scenery studied. In practice, the inversion process is terminated after a certain number L of iterations, and K_{L} is accepted as an approximation for the set K of parameters.

It is desired that at each step the algorithm be closer to the convergence of the solution. The nth iteration, generically, may be written as follows:

(i) Make an initial guess for the set of parameters that one intends to estimate: k_j, $j = 1,\ldots,M$.
(ii) Specify upper and lower bounds, l_j and u_j, of the searched parameters k_j.
(iii) Resolve the forward model, using the forcing variables and the *initial guess*, to calculate heat and radiation fluxes, $C_{L,i}^{calc}(K)$, $C_{S,i}^{calc}(K)$, and $C_{R,i}^{calc}(K)$.
(iv) Compare the computed fluxes $C_{L,i}^{calc}(K)$, $C_{S,i}^{calc}(K)$, and $C_{R,i}^{calc}(K)$ with the measured data $C_{L,i}^{exp}$, $C_{S,i}^{exp}$, and $C_{R,i}^{exp}$, respectively, using Eq. (4).
(v) Minimize Eq. (4) subjected to $l_j \le k_j \le u_j$.
(vi) Convergence test. If the residuals are still larger than a pre-specified value, the solution set obtained becomes the new trial set for the next iteration. With this new set of values, go back to step (iii) and repeat the process. Otherwise, optimization terminates to yield the values of the parameters that give the best fit.

4. Statistical comparison of the results

To evaluate the agreement between simulated and observed fluxes, a statistical comparison is performed using the t-statistic indicator proposed by Stone (1993). This indicator is used along with two other well-known parameters: root-mean-square error (RMSE) and mean-bias error (MBE). Both RMSE and MBE have been especially employed as adjustment indicators of solar radiation models (Halouani et al., 1993; Soler, 1990; Ma and Iqbal, 1984). The RMSE and the MBE are defined as follows

$$\mathrm{RMSE} = \left(\frac{1}{N} \sum_{i=1}^{N} d_i^2 \right)^{1/2} \tag{5}$$

$$\mathrm{MBE} = \frac{1}{N} \sum_{i=1}^{N} d_i \tag{6}$$

Here N is the total number of observations and d_i is the deviation between the ith calculated value and the ith measured value. The test of MBE provides information on the long-term performance of models studied. A positive MBE value gives the average amount of overestimation in the calculated values and vice versa. In general, a small MBE is desirable. It should be noted, however, that overestimation of an individual observation will cancel underestimation in a separate observation. On the other hand, the test on RMSE provides information on the short-term performance of models, as it allows a term-by-term comparison of the actual deviation between the calculated value and the measured value (Halouani et al., 1993). Thus, each test by itself may not be an adequate indicator of a model's performance because it is possible to have a large value for the RMSE and, at the same time, a small value for the MBE, and vice versa.

Therefore, Stone (1993) introduces the t-statistic as a new indicator of adjustment between calculated and measured data. This statistical indicator allows models to be compared

Table 4
Search intervals for the winter experiment

Parameter	Search interval	Reference
z_0 (m)	0.05–0.09	Sutton, 1953
σ_f	0.2–0.8	Oliveira et al., 1998
α_f	0.14–0.45	Burman and Pochot, 1994
ε_f	0.95–0.98	Brutsaert, 1991
ε_g	0.95–0.98	Brutsaert, 1991
w_k	0.1–0.3	Deardorff, 1978
w_{wilt}	0.1–0.5	Deardorff, 1978

and, at the same time, can indicate whether or not a model's estimates are statistically significant at a particular confidence level. Moreover, it can be computed using both the root-mean-square error and mean-bias error and takes into account the dispersion of the results, which is neglected when the root-mean-square error and mean-bias error are considered separately. Although Stone (1993) has employed this test to evaluate the accuracy of the correlations for a solar radiation model, the t-statistic proved to be very efficient when employed by Oliveira et al. (1998) to evaluate the performance of D78. The t-statistic is defined as

$$t = \left(\frac{(N-1)\mathrm{MBE}^2}{\mathrm{RMSE}^2 - \mathrm{MBE}^2} \right)^{1/2} \tag{7}$$

To determine whether a model's estimates are statistically significant, one has simply to determine a critical t_c value obtainable from standard statistical tables, e.g., $t_c(\alpha/2)$ at the α level of significance, and $N-1$ degrees of freedom. For the model's estimates to be judged statistically significant at the $1-\alpha$ confidence level, the calculated value must be between the interval defined by $-t_c$ and t_c (acceptance region under the reduced normal distribution curve). Values outside this interval, the so-called critical region, are those for which we reject the hypothesis that the parameter selection has improved the model.

5. Numerical results

Targino (1999) performed a number of sensitivity studies using D78 and concluded that the model was not significantly sensitive to canopy roughness length z_{0h}, displacement

Table 5
Search intervals for the summer experiment

Parameter	Search interval	Reference
z_0 (m)	0.04–0.2	Oke, 1987
σ_f	0.2–0.8	Oliveira et al., 1998
α_f	0.15–0.25	Sellers, 1965
ε_f	0.98–0.99	Sellers and Dorman, 1987
ε_g	0.95–0.98	Brutsaert, 1991
w_k	0.05–0.3	Deardorff, 1978
w_{wilt}	0.1–0.5	Deardorff, 1978

Table 6
Estimated parameters for the winter experiment

Parameter	Estimated value
z_0 (m)	0.05
σ_f	0.45
α_f	0.35
ε_f	0.95
ε_g	0.95
w_k	0.21
w_{wilt}	0.42

height d, and the soil thermal diffusivity K_s. This way, we reduced the number of parameters to be estimated from 10 (expressed in Table 2) to 7, corresponding to those which are most important to D78 and whose specification are likely to be affected by uncertainties. The other internal parameters related to the soil–vegetation interface were assumed to be similar to Targino (1999): for summer and winter, respectively, $z_{0h} = 0.1$ and 0.06 m; $d = 0.34$ and 0.2 m, which is equal to three fourths of the foliage top height; and $K_s = 2.4 \times 10^{-07}$ and 3.3×10^{-07} m^2 s^{-1}, estimated from measured soil temperature and heat flux profiles.

To initialize the inversion process, one needs to input the first guess values to the optimization algorithm. The choice of a "good" first guess makes the difference between a fast or slow convergence (Bard, 1974). The choice is usually based on previous knowledge of the problem and then on personal intuition.

To carry out this study, a literature review was undertaken to find reference values for the parameters to be estimated. Then, we established upper and lower bounds for each parameter, which correspond to the search intervals of the optimization algorithm, assuring that the algorithm finds physically consistent values. Thus, the first guess is composed of values that belong to the established limits. A compilation of the reference values found is summarized in Tables 4 and 5.

It is important to highlight some points concerning σ_f, w_k and w_{wilt}. Firstly, Oliveira et al. (1998) do not suggest any interval for σ_f; actually, they use the value of 0.25 in their simulations. After many trial-and-error tests, they concluded that this value provided the most suitable representation of the scenarios studied (Oliveira, 2000, personal communication). D78 does not mention intervals for w_k and w_{wilt} either; instead, the suggested values for w_k and w_{wilt} are 0.1 and 0.3, respectively. Due to lack of further information, in

Table 7
Estimated parameters for the summer experiment

Parameter	Estimated value
z_0 (m)	0.09
σ_f	0.35
α_f	0.25
ε_f	0.98
ε_g	0.95
w_k	0.30
w_{wilt}	0.50

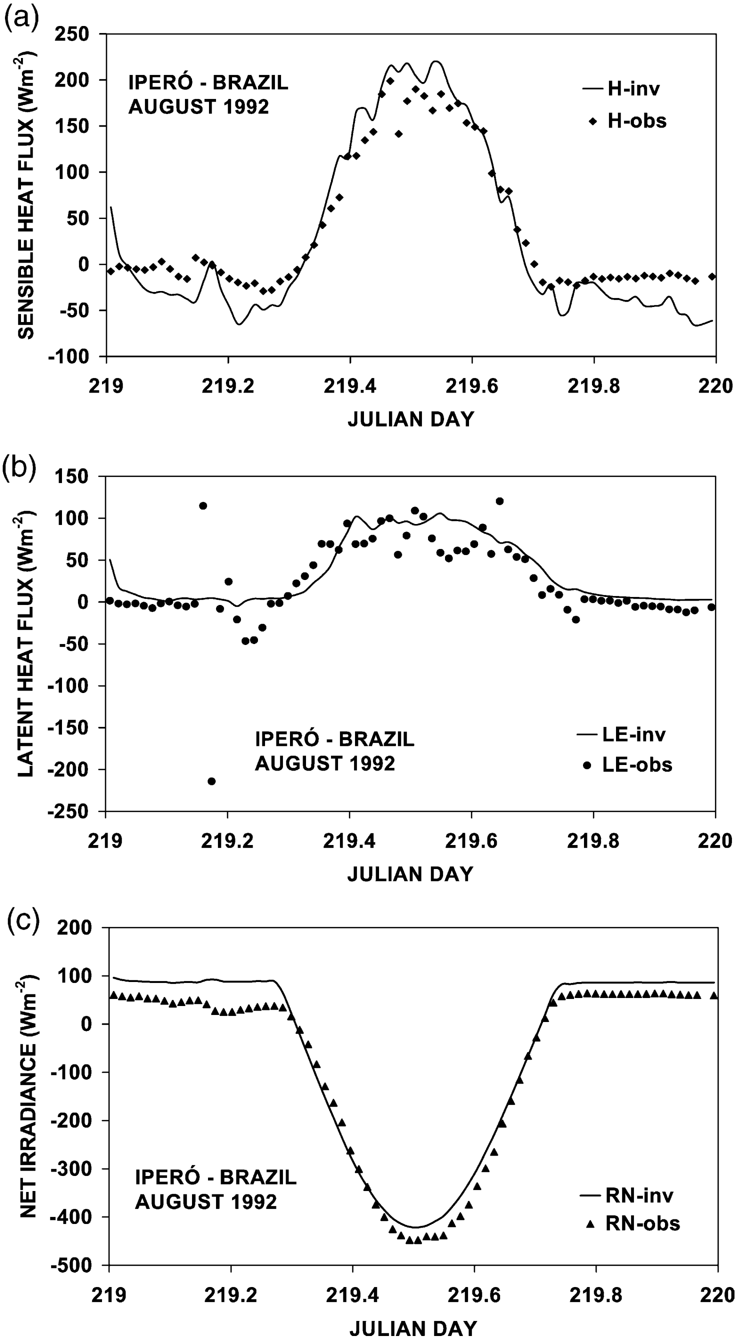

Fig. 3. Observed and modeled fluxes for the winter experiment: (a) sensible heat flux; (b) latent heat flux; (c) net irradiance.

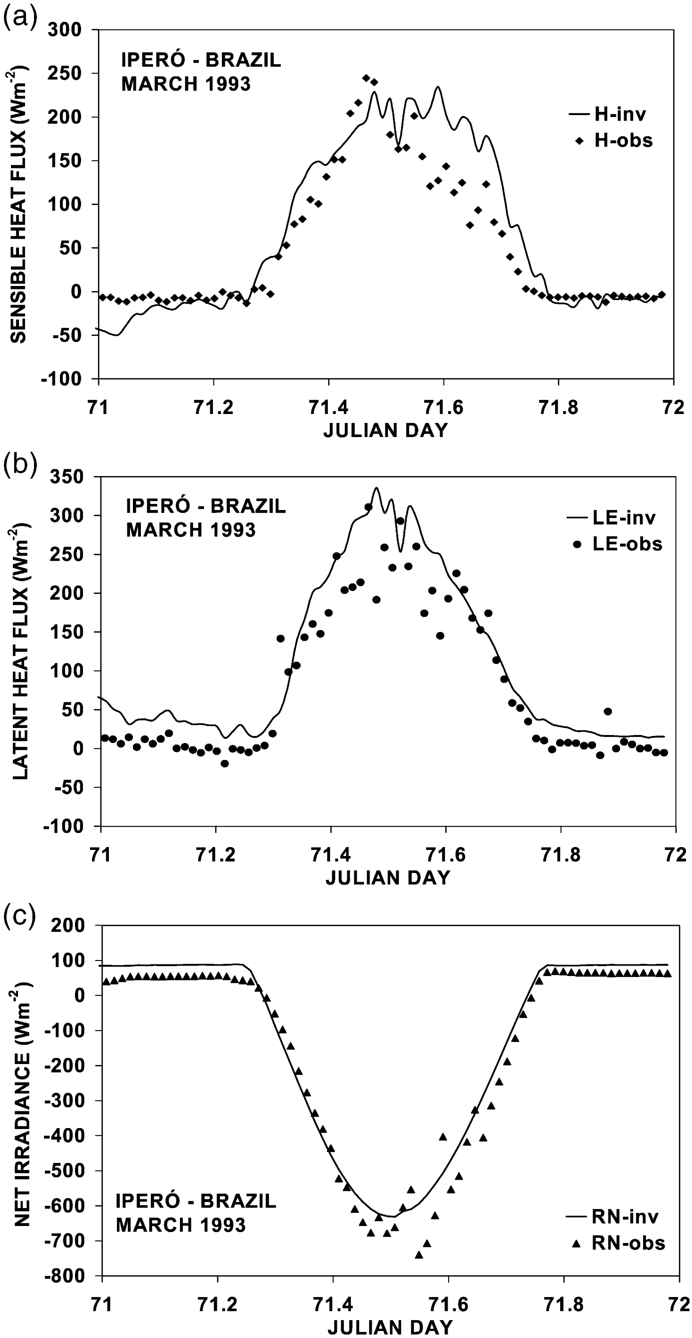

Fig. 4. Observed and modeled fluxes for the summer experiment: (a) sensible heat flux; (b) latent heat flux; (c) net irradiance.

Table 8
Statistical indicators of performance of D78 for winter experiment

Variable	MBE	RMSE	t-Statistic	t_c (all cases)
Hs_{August}	− 6.359	27.634	**1.978**	
LE_{August}	11.898	36.380	**2.896**	3.211
RN_{August}	24.265	32.470	9.410	

the present work these values have been assumed as intermediate values for the corresponding established search interval.

Tables 6 and 7 show the values estimated by the inversion model for both experiments studied. The number of iterations required until convergence was about 250. All values are within the bounds established in Tables 4 and 5. The resulting values listed in Tables 6 and 7 are the "preferred" values that now provide the calibration of D78.

To establish the model's correspondence with observations, simulations have been performed employing the optimized parameters. Figs. 3 and 4 show the diurnal variations of the surface fluxes for both experiments. As can be seen, D78 is able to simulate phase and amplitude of the observed fluxes, presenting the typical patterns: the amplitude of the fluxes being higher in summer than in winter. During the night, the sensible heat flux is negative and the latent heat flux is slightly positive, as expected. The computed sensible heat flux series agrees well with the observations for the winter experiment (Fig. 3a). The computed sensible heat flux shows a somewhat worse agreement with the observed values for the summer experiment (Fig. 4a).

The amplitude of the latent heat flux is much more pronounced in the summer experiment (Fig. 4b) than for the winter experiment (Fig. 3a). Besides the seasonal course of the short-wave radiation flux, the vegetation coverage contributes to this pattern, since there is more moisture available to transform the net irradiance into latent heat flux, compared with the winter experiment. For the net irradiance, the figure shows that the model overestimates the observed values in the morning and shortly after evening, especially for the winter experiment (Fig. 3c). However, it agrees quite well for the convective period. For the summer experiment, the observed net irradiance presents deviations during the convective period, probably due to clouds (Fig. 4c). In this situation, D78 is unable to simulate this physical effect, since the parameterization included in the model to calculate the radiation budget does not take into account clouds effects.

To objectively evaluate whether these model's estimates are statistically significant, i.e., not significantly different from their measured counterparts, we employed the statistical test described in the Section 4. With a degree of freedom equal to 72 and a significance level equal to 0.001, the indicator values printed in Tables 8 and 9 were found.

Table 9
Statistical indicators of performance of D78 for Julian day 71 (summer experiment)

Variable	MBE	RMSE	t-Statistic	t_c (all cases)
$Hs_{March(71)}$	9.834	50.969	**1.645**	
$LE_{March(71)}$	26.657	42.223	6.811	3.211
$RN_{March(71)}$	26.241	48.187	5.432	

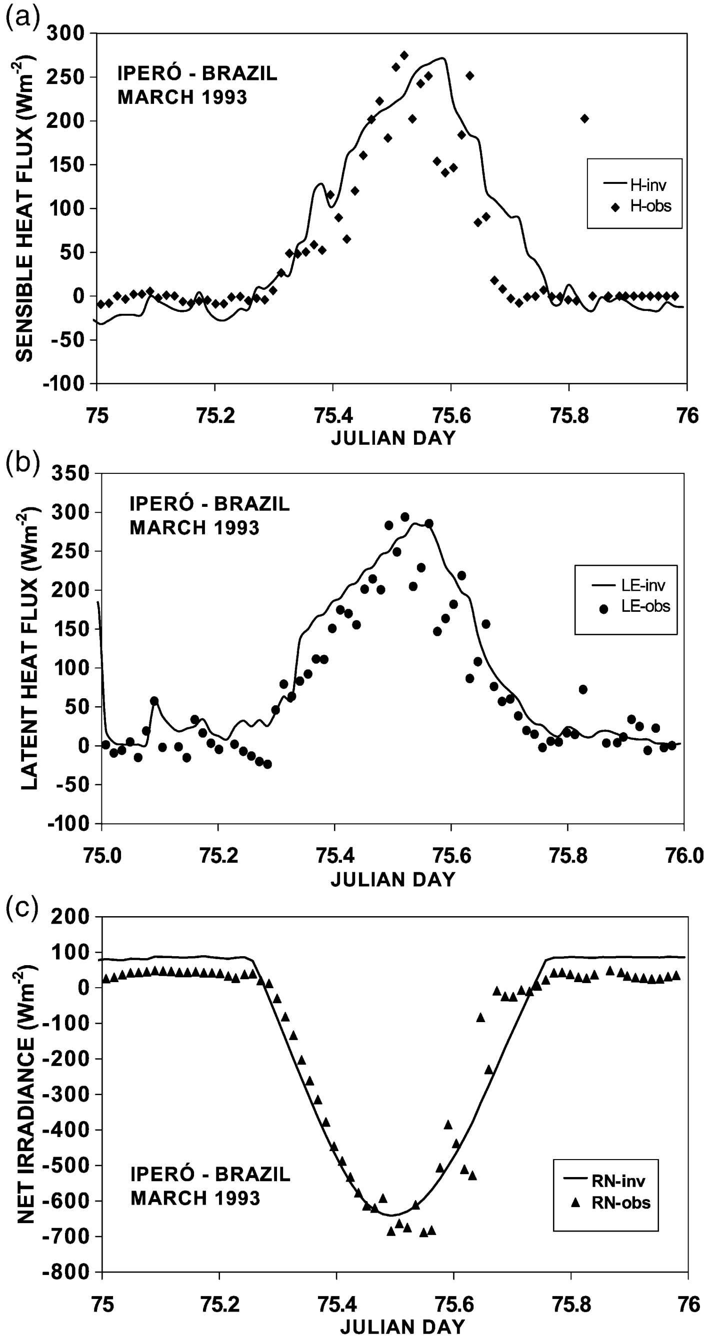

Fig. 5. Observed and modeled fluxes for Julian day 75: (a) sensible heat flux; (b) latent heat flux; (c) net irradiance. The D78 model was run using the same optimized values obtained for the summer experiment (Table 7).

The sensible heat flux series for both experiments, calculated using the optimized parameters, are comparable with observations according to *t*-statistic test, and so is the latent heat flux for the winter experiment. For the summer experiment, the calculated latent heat flux does not agree with the measured latent heat flux according to the *t*-statistic test. This may be due to the overestimation of the calculated series, expressed by the positive MBE. For the net irradiance series, the MBE has more or less comparable values, showing overestimation of the calculated series.

It is worth outlining some features of the forward model that may have driven the overestimation of the MBE of the latent heat flux for the summer experiment. To establish the energy budget for the vegetative layer, D78 assumes that it has no heat capacity. This may be especially important for this experiment, whose surface was covered by corn 50 cm high. The biomass associated with the canopy may hold an important fraction of the energy that closes the energy budget. In this case, it would be important to introduce an energy storage term in the energy budget equation.

For the net irradiance simulations, the shortcomings may be related with the exclusion of a cloud parameterization in the D78 version employed in this study. During the winter simulation the observed net irradiance series presents typical behavior of cloud coverage, for the noon period. Evidently, this is not simulated by the forward model, showing that there is difficulty to model radiative fluxes accurately. The overprediction of the net radiation during the night may be due to the overprediction of the incoming infrared radiation. Unfortunately there were not observations of all the radiative fluxes, otherwise they could have been used as additional information for the inverse model. Thus, the errors of simulation of the radiative fluxes can be compensated by inaccurate adjustments of the parameters.

Since the values estimated by the inversion model should be representative for the area and periods studied, it is important to show the general applicability of the method discussed here. We choose to model another day for the summer period (Julian day 75) and keep unchanged the optimized values shown in Table 7.

Fig. 5 shows the simulations for the sensible and latent heat fluxes and net irradiance. The statistical indicators are printed in Table 10. The agreement between the observed and modeled series are comparable to the summer experiment (Fig. 4). In the case of the sensible heat flux the modeled series is much closer to observations than in Fig. 4a, where the modeled curve overestimated observations in the noon period. The modeled net irradiance fluxes, as in Fig. 4c, presents values between 80 and 100 W m^{-2} larger than the observed values for the night period. This common feature reinforces the idea that the radiation scheme of the direct model lacks the description of important processes, and thus the behavior of the radiation cycle for the night period is not well simulated.

Table 10
Statistical indicators of performance of D78 for Julian day 75

Variable	MBE	RMSE	*t*-Statistic	t_c (all cases)
$Hs_{March(75)}$	9.483	49.845	**1.609**	
$LE_{March(75)}$	20.102	36.665	5.446	3.211
$RN_{March(75)}$	10.699	67.370	**1.336**	

6. Concluding remarks

The main objective of this work was to assess the feasibility of a new approach to obtain a set of representative parameters for calibrating D78.

The optimization process with the D78 model clearly can yield reasonable average values of the free parameters. The optimized values provide encouraging evidence of the applicability of the inversion technique as an alternative method to estimate parameters when there are no reference values available. In the cases studied, the optimization yielded parameter values that corresponded reasonably well with valued suggested in the literature.

Comparisons between observations and model simulations using the optimized parameters indicated that there is an adequate agreement between the series. The best agreement is achieved for the sensible heat flux and the worst for net irradiance, according to the statistical test employed to evaluate the simulations.

It is important to mention that the main drawbacks found in the simulations may be especially due to the forward model formulation rather than to the inversion model. This may be the case of the latent and net irradiance fluxes, whose results are presumably affected by the lack of some important details in the parameterization, as discussed in the previous section.

Those considerations would lead to improvements in the results of the inversion algorithm.

Acknowledgements

This research was supported by a grant sponsored by CAPES/Brazil while the first author was developing his Master's dissertation at the Department of Atmospheric Sciences, University of São Paulo (USP), Brazil. The second author thanks the support of CNPq Grant No. 300040/94-6 (NV). The authors are grateful to Dr. Haroldo Velho and MSc Marcelo Moraes, from LAC/INPE, who provided useful comments and tips about the inversion code, and Dr. Amauri Pereira de Oliveira from USP, for supplying the experimental data. The authors acknowledge the anonymous reviewers for their valuable comments and suggestions for improvement of the manuscript.

References

André, J.C., Goutorbe, J.P., Perrier, A., 1986. HAPEX-MOBILHY: a hydrologic atmospheric experiment for the study of water budget and evaporation flux at the climate scale. Bull. Am. Meteorol. Soc. 67, 138–144.

Anthes, R.A., 1984. Enhancement of convective precipitation by mesoescale variations in vegetative covering in semiarid regions. J. Clim. Appl. Meteorol. 23, 541–554.

Bard, Y., 1974. Nonlinear Parameter Estimation. Academic Press, New York, 341 pp.

Barnes, S.L., 1964. A technique for maximizing details in numerical weather map analysis. J. Appl. Meteorol. 3, 396–409.

Bhumralkar, C.M., 1975. Numerical experiments on the computation of ground surface temperature in an atmospheric general circulation model. J. Appl. Meteorol. 14, 1246–1258.

Blackadar, A.K., 1976. Modeling the nocturnal boundary layer. Proceedings of the Third Symposium on Atmospheric Turbulence, Diffusion and Air Quality. American Meteorological Society, Boston, MA, pp. 46–49.

Bougeault, P., 1991. Parameterization schemes of land-surface process for mesoescale atmospheric models. Land Surface Evaporation: Measurements and Parameterization. Spring-Verlag, New York, pp. 55–92.
Brutsaert, W., 1991. Evaporation into the Atmosphere: Theory, History and Application. Kluwer Academic Publishing, Dordrecht, 299 pp.
Burman, R., Pochot, L.O., 1994. Evaporation, Evapotranspiration and Climatic Data Elsevier, Amsterdam, 278 pp.
Deardorff, J., 1978. Efficient prediction of ground surface temperature and moisture with inclusion of a layer vegetation. J. Geophys. Res. 83 (C4), 1899–1903.
Garrett, A.J., 1982. A parameter study of interactions between convective clouds, the convective boundary layer, and a forested surface. Mon. Weather Rev. 110, 1041–1059.
Halouani, N., Nguyen, C.T., Vo-Ngoc, D., 1993. Calculation of monthly average global solar radiation on horizontal surfaces using daily hours of bright sunshine. Solar Energy 50 (3), 247–258.
Idso, S.B., Jackson, R.D., Reginato, R.J., Kimball, B.A., Nakayama, F.S., 1975. The dependence of bare albedo on soil water content. J. Appl. Meteorol. 14, 109–113.
Jacquemin, B., Noilhan, J., 1990. Sensitivity study and validation of land surface parameterization using the HAPEX-MOBILHY data set. Boundary-Layer Meteorol. 52, 93–134.
Ma, C.C.Y., Iqbal, M., 1984. Statistical comparison of solar radiation correlations. Monthly average global and diffuse radiation on horizontal surfaces. Solar Energy 33 (2), 143–148.
McCumber, M.C., 1980. A numerical simulation of the influence of heat and moisture fluxes upon mesoescale circulation, PhD Thesis, University of Virginia, USA, 255 pp.
McCumber, M.C., Pielke, R.A., 1981. Simulation of the effects on surface fluxes of heat and moisture in a mesoescale numerical model: Part 1. soil layer. J. Geophys. Res. 86, 9929–9938.
Mihailovic, D.T., De Bruin, H.A.R., Jeftic, M., Van Dijken, A., 1992. A study of the sensitivity of land surface parameterization to the inclusion of different fractional covers and soil textures. J. Appl. Meteorol. 31, 1477–1487.
Mihailovic, D.T., Kallos, G., 1997. A sensitivity study of a coupled soil–vegetation boundary-layer scheme for use in atmospheric modeling. Boundary-Layer Meteorol. 82, 287–315.
Numerical Algorithms Group (NAG) Fortran E04UCF Routine Document, 1993. Library Mark 16. Oxford, UK, 33 pp. (document also available via www as http://www.nag.co.uk/numeric/FL/manual/pdf/E04/e04ucf.pdf).
Oke, T.R., 1987. Boundary Layer Climates, 2nd edn. Methuem, London, 435 pp.
Oliveira, A.P., 1993. Estudo da dinâmica da camada limite planetária em latitudes tropicais e subtropicais. Technical Report (in Portuguese), Department of Atmospheric Sciences, University of São Paulo, Brazil, 70 pp.
Oliveira, A.P., Soares, J., Tirabassi, T., Rizza, U., 1998. A surface energy-budget model coupled with a skewed puff model for investigating the dispersion of radionuclides in a sub-tropical area of Brazil. Il Nuevo Cemento 21C, 631–647.
Ookouchi, Y., Segal, M., Kessler, R.C., Pielke, R.A., 1984. Evaluation of soil moisture effects on the generation and modification of mesoescale circulations. Mon. Weather Rev. 112, 2281–2292.
Sellers, W.D., 1965. Physical Climatology. Univ. of Chicago Press, Chicago, p. 272.
Sellers, P.J., Dorman, J.L., 1987. Testing the simple biosphere model (SiB) using a point micrometeorological and biophysical data. J. Clim. Appl. Meteorol. 26, 622–651.
Sellers, P.J., Mintz, Y., Sud, Y.C., Dalcher, A., 1986. A simple biosphere model (SiB) for use within general circulations models. J. Atmos. Sci. 43, 505–531.
Sellers, P.J., Shuttleworth, W.J., Dorman, J.L., Dalcher, A., Roberts, J.M., 1989. Calibrating the simple biosphere model for amazonian tropical forest using field and remote sensing data: Part 1. Average calibration with field data. J. Appl. Meteorol. 28, 727–759.
Shukla, J., Mintz, Y., 1982. Influence of land-surface evapotranspiration on the Earth's climate. Science 215, 1498–1500.
Soares, J., Oliveira, A.P., Escobedo, J.F., 1996. Surface energy balance observation and numerical modeling applied to Candiota. Air Pollution and Acid Rain: the Candiota Program. Bauru, Brazil, pp. 68–77.
Soler, A., 1990. Statistical comparison for 77 European stations of 7 sunshine-based models. Solar Energy 45 (6), 365–370.
Stone, R.J., 1993. Improved statistical procedure for the evaluation of solar radiation estimation models. Solar Energy 51 (4), 289–291.

Sutton, O.G., 1953. Micrometeorology. McGraw-Hill Book Company, 333 pp.

Targino, A.C., 1999. Modelagem de balanços de energia para Iperó (SP): uma abordagem utilizando metodologia de inversão, Master's Dissertation (in Portuguese), Department of Atmospheric Sciences, University of São Paulo, Brazil, 107 pp.

Woodbury, K.A., 1995. What are inverse problems? Hypertext document available via www as http://www.me.ua.edu/inverse/whatis html.